ACS SENSORS

pubs.acs.org/acssensors

Article

Deep-Learning-Guided Electrochemical Impedance Spectroscopy for Calibration-Free Pharmaceutical Moisture Content Monitoring

Guangshuai Han, Brent Maranzano, Christopher Welch, Na Lu, and Yining Feng*

Cite This: *ACS Sens.* 2024, 9, 4186−4195

Read Online

ACCESS | Metrics & More | Article Recommendations | Supporting Information

ABSTRACT: The moisture content of pharmaceutical powders can significantly impact the physical and chemical properties of drug formulations, solubility, flowability, and stability. However, current technologies for measuring moisture content in pharmaceutical materials require extensive calibration processes, leading to poor consistency and a lack of speed. To address this challenge, this study explores the feasibility of using impedance spectroscopy to enable accurate, rapid testing of moisture content of pharmaceutical materials with minimal to zero calibration. By utilizing electrochemical impedance spectroscopy (EIS) signals, we identify a strong correlation between the electrical properties of the materials and varying moisture contents in pharmaceutical samples. Equivalent circuit modeling is employed to unravel the underlying mechanism, providing valuable insights into the sensitivity of impedance spectroscopy to moisture content variations. Furthermore, the study incorporates deep learning techniques utilizing a 1D convolutional neural network (1DCNN) model to effectively process the complex spectroscopy data. The proposed model achieved a notable predictive accuracy with an average error of just 0.69% in moisture content estimation. This method serves as a pioneering study in using deep learning to provide a reliable solution for real-time moisture content monitoring, with potential applications extending from pharmaceuticals to the food, energy, environmental, and healthcare sectors.

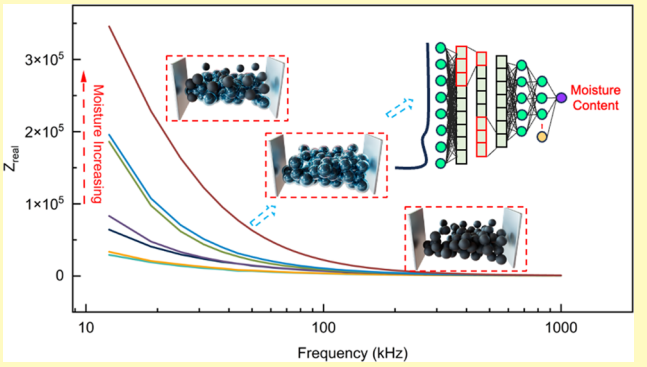

KEYWORDS: *electrochemical impedance spectroscopy, moisture sensing, equivalent circuit modeling, 1D convolutional neural network, pharmaceutical industry*

In the pharmaceutical industry, precise moisture monitoring in raw materials is essential for both quality assurance and patient safety, ensuring streamlined production and significant cost efficiencies.[1−5] Therefore, monitoring the raw materials of pharmaceutical drugs is a crucial step in the production process.[6,7] However, the methods available for real-time moisture content monitoring are highly limited.[8−10] Common techniques for moisture content detection possess various limitations, making in-line water content monitoring extremely challenging.[11−13] For instance, near-infrared (NIR) spectroscopy requires calibration for different materials, which adds complexity and time-consuming steps to the process.[14−16] Moreover, NIR measurements are not sufficiently accurate in determining the water content. Karl Fischer titration, while accurate for detecting water content in pharmaceuticals, poses a significant time requirement and is unsuitable for implementation on a production line. As a result, much of the research focuses on streamlining the testing process to reduce time consumption.[17−19] Impedance spectroscopy serves as a potent sensing technique suitable for real-time, non-invasive process parameter control, thus finding application in monitoring the status of various samples, such as pharmaceuticals, soils, crops, and food products.[20−25] For instance, Ando et al. utilized equivalent circuit analysis and other methods to interpret the relationship between impedance spectra and the drying conditions of the sample.[26−29] Cheng et al. conducted dielectric measurements on pharmaceutical drugs with varying concentrations and discovered that the dielectric constant could potentially serve as an indicator for monitoring the dosage of the drug.[30] However, most of these similar studies have been primarily focused on demonstrating the feasibility of using impedance/dielectric spectroscopy as a method for monitoring sample moisture content with limited discussions on the development of models to determine sample moisture content based on test data in a concise manner. Furthermore, there is a notable lack of research specifically addressing pharmaceutical raw materials in this context.[31−33] This gap in research underscores the need for comprehensive models and

Received: May 16, 2024
Revised: July 23, 2024
Accepted: July 29, 2024
Published: August 3, 2024

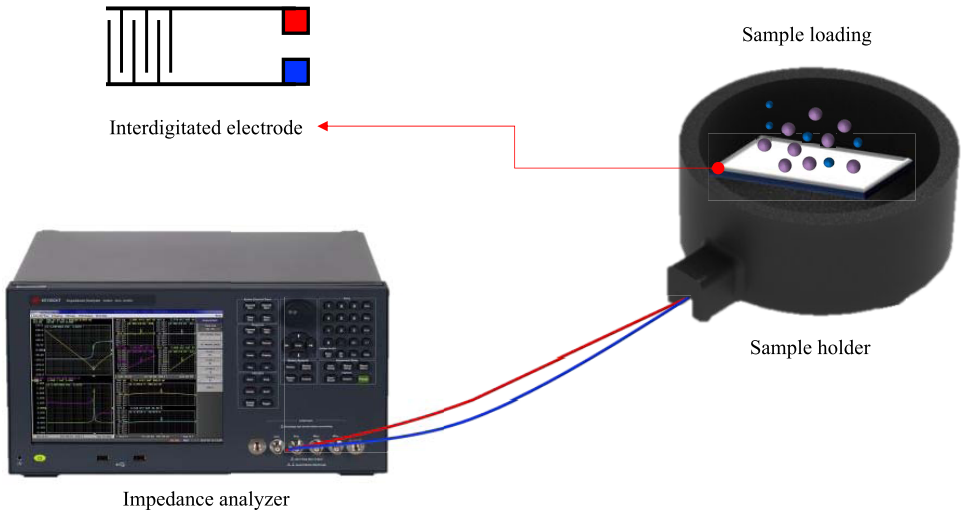

Figure 1. Experimental setup for the measurement of the electrical signal.

tailored approaches, especially considering the critical role of moisture content in determining the quality, efficacy, and safety of pharmaceutical products.[34−38]

Therefore, this study aims to provide an accurate and efficient method for real-time moisture content monitoring in pharmaceuticals with minimal to zero calibration. We utilized electrochemical impedance spectroscopy (EIS) to measure the electrical properties of pharmaceutical materials under various moisture conditions. EIS effectively discerns the physical properties from electrical characteristics, revealing the intricate relationship between signal behavior and real-time physical characteristics of the samples.[39−42] Initially, a statistical analysis explored the correlation between EIS signals and moisture content. Additionally, electrochemical simulation sheds light on the underlying mechanism of moisture monitoring via EIS signals. To enhance the accuracy and effectiveness of moisture content monitoring, we propose the utilization of big data[43,44] and deep learning techniques,[41,42,45−47] 1D convolutional neural network (1DCNN) for signal processing, and the development of a predictive model.[48] Due to the prevalence of AI technologies, deep learning has proven to make outstanding contributions across different disciplines.[49−52] The choice of 1DCNN is driven by its excellence in handling time-series data and extracting key features from complex signals, ideal for EIS data interpretation. In the deep learning process, we introduce an innovative concept called the baseline mechanism, which enables the model to learn the chemical, physical, and electrical information contained in the signals. By incorporation of these multiple dimensions of information, the model can accurately predict the moisture content of pharmaceutical samples, offering a calibration-free, direct measurement that adapts to various sample types and conditions.

EXPERIMENTAL PROGRAM

Sample Preparation. In the experimental project, we selected four common pharmaceutical raw material powders for testing, including MCC (microcrystalline cellulose from AVICEL PH-200), ASP (aspirin, from Sigma-Aldrich), PVA (PVA, Mw 89,000−98,000, 99+% hydrolyzed, from Sigma-Aldrich), and MA (mannitol, PEARLITOL 160 C mannitol, from Roquette). To alter the moisture content of these materials, the samples were mixed with deionized water and then placed in separate chambers under different humidity conditions. The humidity levels varied over a substantial range from 0 to 15%. Once the samples were adequately prepared, they were subjected to further testing under varying humidity conditions.

Moisture Sensing Setup and Validation. In our experimental setup, moisture content and electrical responses of pharmaceutical samples were measured using the Keysight Technologies E4990A impedance analyzer with commercial interdigitated gold electrodes on a custom 3D-printed holder, ensuring precise signal acquisition. Concurrently, the moisture content was validated using the Mettler Toledo HE73 moisture analyzer. The samples were contacted to the analyzer via interdigitated gold electrodes, which have proven to be highly compatible with pharmaceutical and biomedical materials.[20,25] These configurations are illustrated in Figure 1. More detailed information on testing setup can be found in the Supporting Information, S1.

Signal Processing. After the electrical signal and moisture content data of the samples were collected, a statistical approach was employed to assess the variations in the electrical signals at different moisture levels compared to the signals obtained under dry conditions. The root-mean-square deviation (RMSD)[53,54] was utilized as a statistical index for this comparison, specifically to calculate the difference from the baseline spectra. The equation of the RMSD sensing index is shown below in eq 1

$$\mathrm{RMSD}\ (\%) = \sqrt{\frac{\sum_{i=1}^{N} (G_i - G_{\mathrm{bl}})^2}{\sum_{i=1}^{N} (G_{\mathrm{bl}})^2}} \tag{1}$$

where G_i is the spectra of samples of various moisture levels, G_{bl} is the baseline spectra obtained at the dry stage, and N is the data points in the spectra, respectively.

In addition to the statistical analysis, the study also employed EIS and equivalent circuit modeling to analyze the signals. The equivalent circuit consisted of a series resistor (R_s), a parallel resistor (R_p), and a parallel constant phase element (CPE, $Z_{\mathrm{CPE}} = \frac{1}{Q^*(j\omega)^{\alpha}}$, Q is the magnitude of the CPE, ω is the angular frequency, j is the unit of imaginary numbers, α is the phase constant, with its value ranging between 0 and 1). After the fitting process, EIS indices, R_index (represents the resistance parameter derived from the parallel resistor in the equivalent circuit model fitting, herein referred to as R_index), Q_index (corresponds to the charge parameter from the CPE, herein referred to as Q_index), and α_index (denotes the phase parameter of the CPE component, herein referred to as α_index) were calculated based on the equivalent circuit parameters obtained from the model. Thus, the measured signal can be expressed by the eq 2

$$Z = Z' + Z'' = R_s + \frac{1}{\left(1/R_p\right) + Z_{\mathrm{CPE}}} \tag{2}$$

https://doi.org/10.1021/acssensors.4c01180
ACS Sens. 2024, 9, 4186−4195

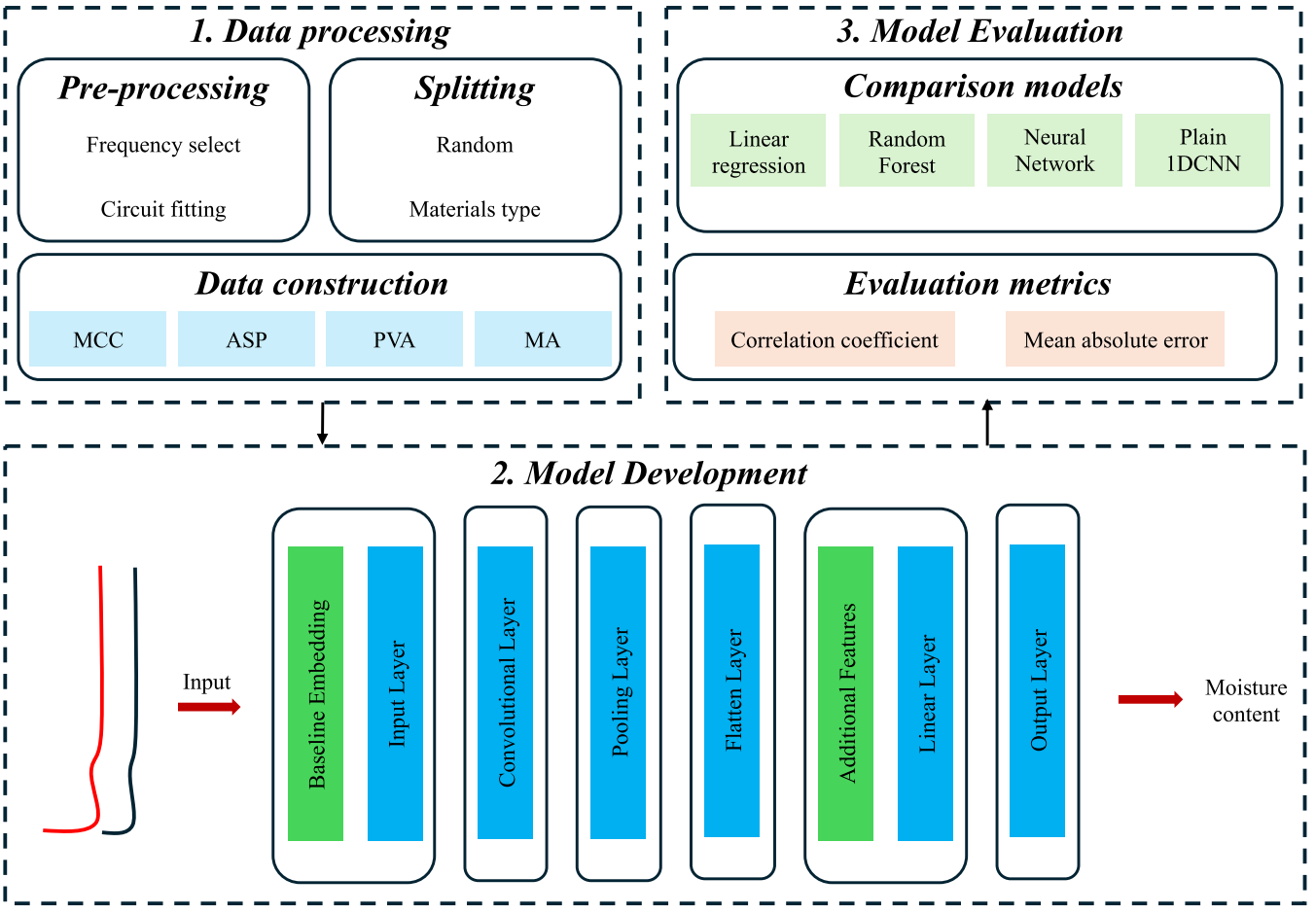

Figure 2. Schematic of the proposed deep learning framework for data-driven moisture content sensing.

where Z' is the real part of the spectroscopy and Z'' is the imaginary part of the spectroscopy. The calculated EIS indices were then utilized to establish a correlation with the moisture content of pharmaceutical samples, aiming to elucidate the mechanism by which EIS signals can sense the moisture content.

Moisture Content Sensing Model Development. We introduce the innovative approach proposed in this study, which utilizes a 1DCNN model to establish a moisture content evaluation model, as illustrated in Figure 2 schematic of the proposed deep learning framework for data-driven moisture content sensing. The 1DCNN model has been widely used for processing spectrum-type signals and has shown promising results in various signal analysis tasks.[55,56] The data processing includes frequency selection, circuit fitting, and data construction from four commonly used pharmaceutical materials (MCC, ASP, PVA, and MA) recommended by our industry partner for pilot testing. The model's robustness is evaluated using two different data splitting methods and compared with several baseline machine learning models and data processing techniques. Additionally, the physical and chemical properties of the powders are incorporated as additional features into the 1DCNN structure to enhance the model's accuracy in moisture content prediction. Detailed information regarding the model's parameters, training process, and comparative analysis of model performance is available in Supporting Document S2.

RESULTS AND DISCUSSION

Impedance Spectroscopy Analysis. Figure 3a demonstrates the changes in electrical signals of the MCC powder as a representative material in response to varying moisture contents. An observable trend is observed where the real part of the EIS signal increases with an augmentation in moisture content. This phenomenon indicates that the electrical properties of the material system within the sample are significantly influenced by changes in moisture content, which is clearly reflected in the EIS measurements. Figure 3b presents the changes in the imaginary part of the EIS signal, demonstrating a distinct response corresponding to the variation in the moisture content. The alterations in both the real and imaginary components of the EIS signal affirm that the spectroscopy of the pharmaceutical material can be effectively employed to track and monitor changes in the moisture content of the samples. The observed sensitivity of the EIS signals to changes in moisture content highlights its potential as an accurate and rapid method for real-time moisture content monitoring in pharmaceutical production processes.

To quantitatively characterize the relationship between signal changes and moisture content, the RMSD index (from eq 1) is employed to assess how the electrical signals of the pharmaceutical material perform under varying moisture content conditions compared to the signals observed under dry conditions. Figure 3c displays the RMSD index calculated within the frequency range 100−1000 kHz, demonstrating a gradual increase in the index as the moisture content rises. This observation signifies that the RMSD index effectively captures the differences in the electrical signals corresponding to different moisture content levels. The RMSD index sensing performance for the rest of the pharmaceutical materials is displayed in the supporting document, Figure S1. Furthermore, the RMSD index exhibits a positive correlation with the actual

https://doi.org/10.1021/acssensors.4c01180
ACS Sens. 2024, 9, 4186−4195

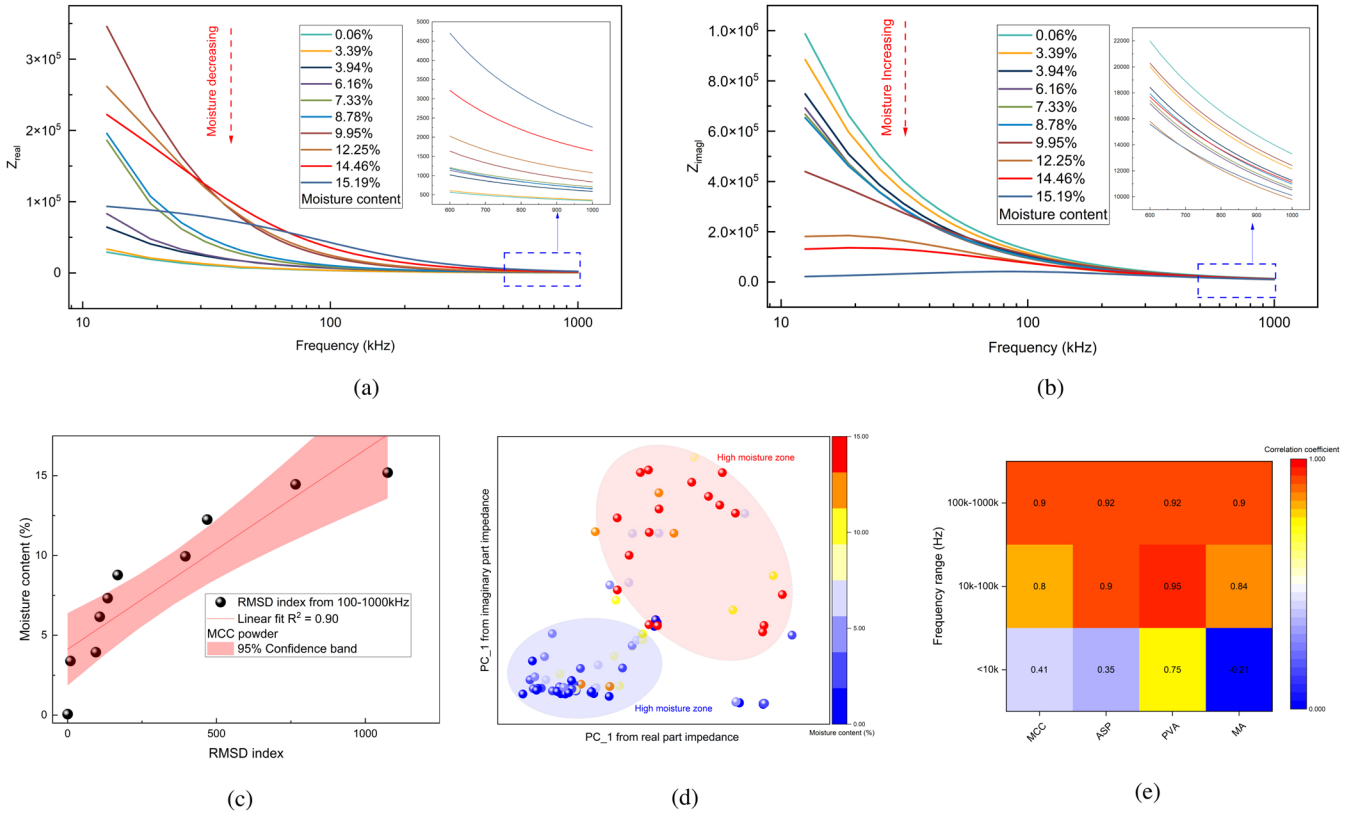

Figure 3. (a) Real part impedance spectroscopy of the representative sample; (b) imaginary part impedance spectroscopy of representative sample; (c) RMSD sensing index vs moisture content at the frequency of 100−1000 kHz; and (d) principal component analysis (PCA) plot using the first principal components (PC_1) of the real and imaginary parts of the impedance spectra, colored by moisture content. (e) Heat map of the correlation coefficient between moisture content and the spectroscopy at different frequencies.

moisture content of the samples, with a correlation coefficient of 0.9. This strong correlation highlights the capability of the RMSD index to accurately represent and quantify the variations in moisture content within the pharmaceutical samples. In addition, we have adopted principal component analysis (PCA) to better illustrate the relationship between the impedance spectrum and the pharmaceutical's corresponding moisture content. By visualizing the dimensionally reduced spectrum information, as shown in Figure 3d, we can observe that the pharmaceutical samples with different levels of moisture content can be separated into two distinct zones. This signifies the sensitivity of the impedance spectrum to the moisture content. However, some data points are located in different areas, which might be attributed to other sample characteristics such as particle size.

In Figure 3e, a comparative analysis of the correlation coefficients between the moisture content and the RMSD index for different sample materials is presented across various frequency ranges. Remarkably, the frequency range of 100−1000 kHz consistently exhibits a stable and robust capacity to describe the changes in moisture content within the samples. It can be observed that frequencies above 10 kHz exhibit a more significant relationship between the signal and moisture content. The utilization of the RMSD index provides a quantitative means to evaluate the relationship between electrical signals and moisture content accurately. The strong correlation observed between the RMSD index, and the actual moisture content supports its potential as a key parameter for the development of the predictive model using deep learning techniques.

Equivalent Circuit Modeling. After performing statistical analysis, equivalent circuit fitting was employed to elucidate the relationship between changes in electrical signals and the moisture content. The purpose of equivalent circuit fitting is to utilize electrochemical impedance to reflect the molecular structure and chemical composition of materials through an electrical model.[39] The mechanism of electrochemical detection, similar to existing studies,[57,58] relies on the interaction between the electrical properties of the sample and its moisture content. The capacitive and resistive elements of the system are influenced by the level of moisture, which affects the impedance measurements. This method is particularly effective because the presence of moisture changes the dielectric properties of the material, which, in turn, affects the impedance.

In this context, the sensor and the pharmaceutical materials can be regarded as resistors within the circuit, while the air between the powder particles and the varying moisture content can be considered as capacitors capable of accumulating charge. Due to the presence of different interfaces, the constant phase element (CPE) was selected as a replacement for the traditional capacitor in the circuit simulation. We discovered that the modeling parameters Q_index and α_index from the CPE demonstrate a strong correlation with the moisture content in pharmaceutical samples. Under dry conditions, the electrical response of the sample resembles an equivalent circuit composed of a capacitor and resistor with the α_index exponent of the CPE component approaching 1. As moisture is introduced, a portion of the sample containing water and air can be represented by an imperfect capacitor using the CPE

https://doi.org/10.1021/acssensors.4c01180
ACS Sens. 2024, 9, 4186−4195

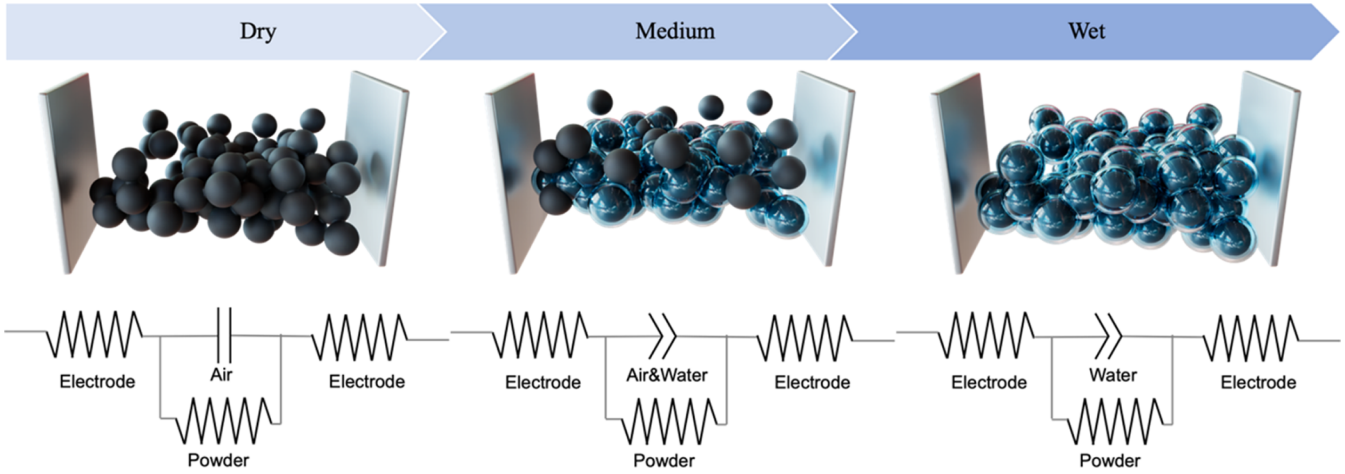

Figure 4. Schematic of the moisture sensing theory.

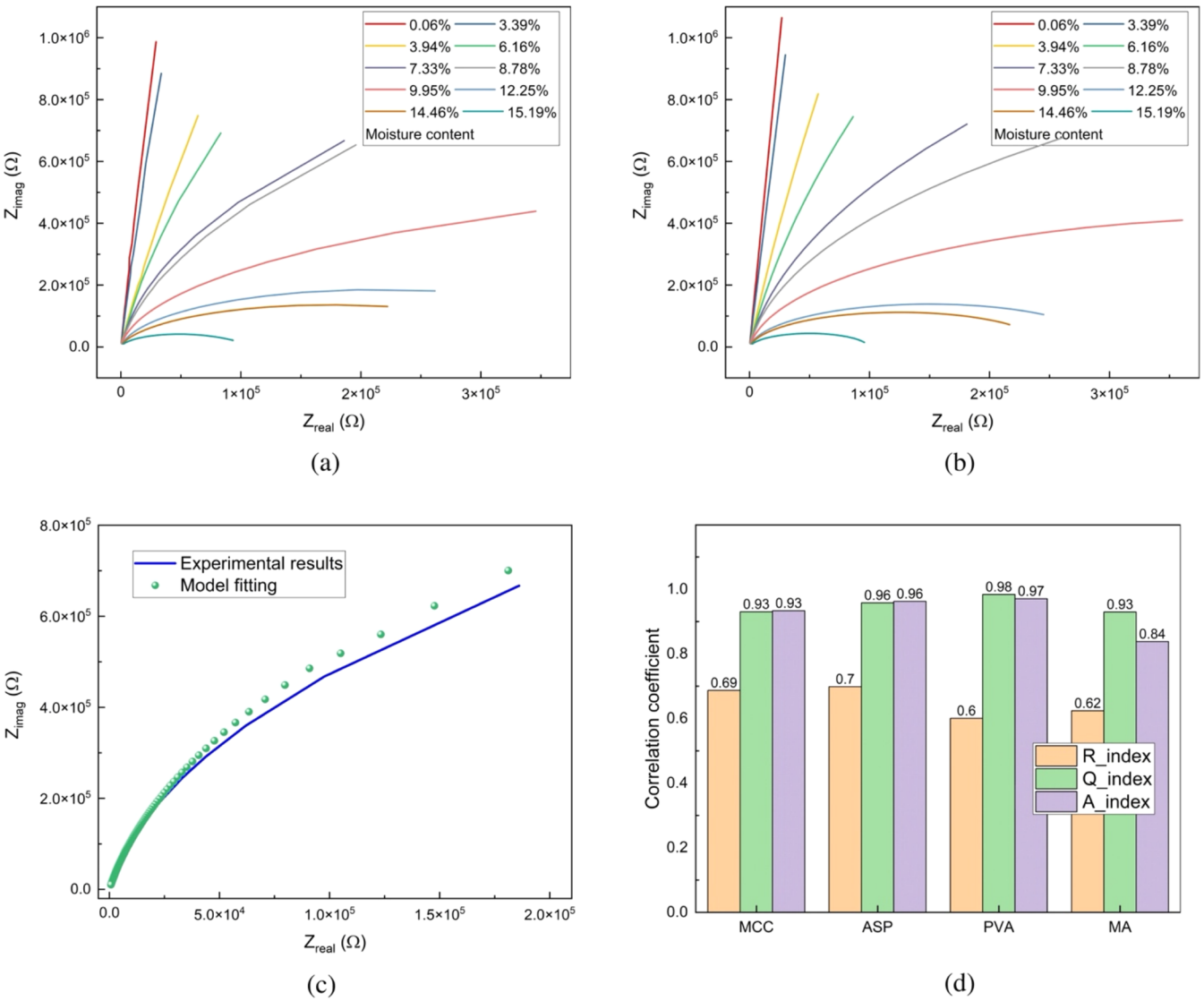

Figure 5. (a) Nyquist plot of the representative MCC powder at different moisture contents; (b) modeling Nyquist plot of the representative MCC powder at different moisture contents; (c) representative equivalent circuit model fitting performance of the MCC powder at the moisture content of 7.33%; and (d) correlation coefficient between the EIS sensing indices and moisture content of various powders. Here, the R index represents the resistance parameter derived from the parallel resistor in the equivalent circuit model fitting. Q_index corresponds to the charge parameter from the constant phase element (CPE), and α_index denotes the phase parameter of the CPE component.

https://doi.org/10.1021/acssensors.4c01180
ACS Sens. 2024, 9, 4186−4195

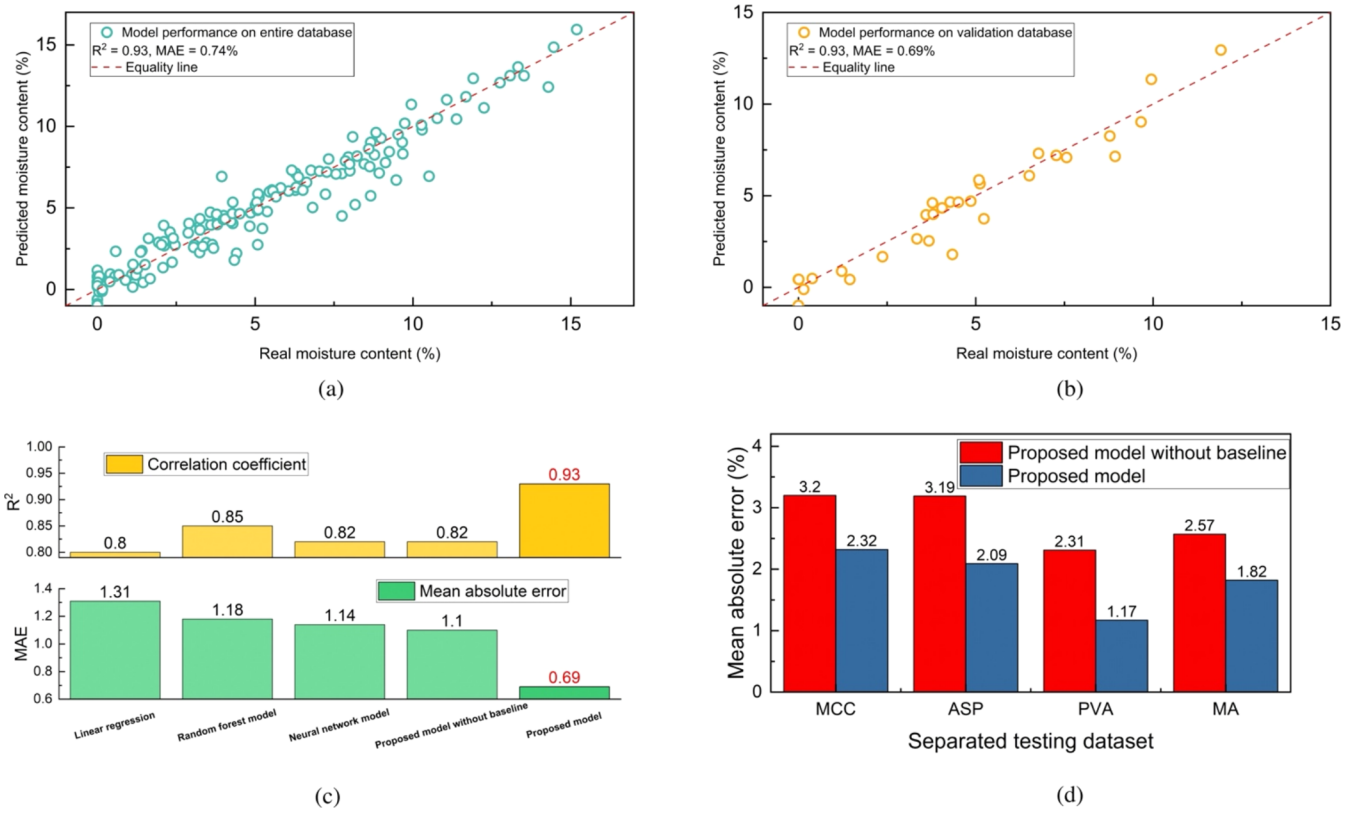

Figure 6. (a) Real moisture content vs predicted moisture content from the entire data set; (b) real moisture content vs predicted moisture content from the validation data set; and (c) comparative performance analysis of moisture content prediction models. The bar charts display R^2 values and mean absolute errors (MAE) for various models, highlighting the enhanced accuracy and correlation of the 1DCNN with baseline mechanism (indicated by the red outlines) over other tested algorithms. (d) Validation performance on different material types. The bar chart compares the mean absolute error percentages of the proposed model with and without the baseline across various materials, highlighting the improved accuracy when the baseline is employed.

element. This process is depicted in Figure 4. To establish a relationship between the electrical signals and moisture content, this study proposes the use of an equivalent circuit, as illustrated in Figure 4, to fit the Nyquist plot data and reveal the mechanism of electrical signal sensing for the moisture content. Figure 5a,b compares the fitted data with experimental data using MCC powder as a representative example, demonstrating that the fitted data accurately represents the variations in moisture content within the samples. This proves that the fitted data can still track the moisture content variation as the real experimental data. To further validate the fitting performance, we selected one of the representative samples, MCC, at 7.33% moisture content, as shown in Figure 5c, demonstrating good agreement between the real and fitted data. This indicates that the proposed equivalent circuit model effectively characterizes the electrical behavior of pharmaceutical samples under different moisture content conditions. The fitting performance for the other three types of samples is illustrated in the supporting document, Figures S2 and S3.

It is observed that the Q_index (a parameter representing the accumulation of charge during the testing process) and α_index (a parameter representing the difference between CPE behavior and a regular capacitor) exhibit high correlation coefficients with the moisture content of the samples. Specifically, the Q_index can be considered to reflect the amount of accumulated charge during the testing process. As the moisture content increases, the presence of water, which can accumulate more charge than air, leads to higher Q-index values, thereby reflecting the moisture content of the samples. On the other hand, the α_index indicates the deviation of the CPE element from a regular capacitor. As the moisture content increases, the CPE behaves less like a normal capacitor, resulting in a decrease in the α_index. The moisture content sensing performance for four types of pharmaceutical materials can be found in the supporting document, Figure S4. By analyzing the Q_index and α_index derived from the equivalent circuit fitting, it becomes possible to estimate the moisture content in pharmaceutical materials based on their electrical responses. The high correlation observed between these indices and the moisture content further validates the effectiveness of the proposed calibration-free approach for real-time moisture content monitoring in pharmaceutical production processes.

Deep-Learning-Based Moisture Content Sensing Model. Despite the high correlation coefficients observed between moisture content and the indices derived from statistical analysis and equivalent circuit fitting, these methods have shown limitations in adaptability across different sample types and sensitivity changes upon sensor replacement. We have also identified that the different particles have varying particle sizes, and this physical property will also affect the electrical performance of the sample and, consequently, the sensing performance. Detailed particle size analysis can be found in the supporting document, Section S3 and Figure S5. As illustrated in Figure S6, the correlation coefficient heat map when data from various sample types and sensors are

https://doi.org/10.1021/acssensors.4c01180
ACS Sens. 2024, 9, 4186−4195

combined shows that the highest correlation coefficient observed is around 0.8. This is significantly lower compared to the nearly 0.95 correlation coefficient achieved with single sample data. This discrepancy highlights the need for a more sophisticated signal processing method and a robust data-driven approach. By leveraging a 1DCNN, we aim to process complex data sets more effectively, enabling calibration-free moisture content sensing that enhances consistency and speeds up analysis in pharmaceutical materials. The detailed installation of the input features can be found in Section 2 of the Supporting Document. Our preliminary analysis of the input features, which is elaborated upon in Sections 3 and 4 of the Supporting Documents, uncovered that some of the selected features exhibit a good correlation with the moisture content, with correlation coefficients ranging from 0.6 to 0.8. This range indicates a substantial relationship, affirming the relevance of our feature selection. Nonetheless, it was apparent that the adoption of a more sophisticated processing technique could reveal deeper insights and potentially enhance the predictive accuracy.

The data set used in the training process consisted of EIS signals from four different pharmaceutical materials with varying particle sizes and moisture contents. Prior to training, the data set was divided into training and validation sets to ensure robust model performance. The 1DCNN model initially separates the baseline signal (corresponding to the sample under dry conditions) and the real-time signals (corresponding to the sample under different humidity conditions) into two layers and feeds them into convolutional layers. Through the convolution, pooling, and flattening processes, the signals are processed and then combined with the physical information on the samples in the fully connected layer. This integration of electrical and physical information enables the model to capture the complex relationship between the input signals and the moisture content. During the training process, the model gradually converged after approximately 100 epochs, as shown in Figure S7 from the Supporting Information. The convolutional and pooling layers play crucial roles in extracting relevant information and reducing the dimensionality of the high-dimensional EIS signals. This allows for effective fusion of the high-dimensional signals with other physical information, providing a conducive environment for the model to better understand the input information and to evaluate the moisture content accurately. Figure 6a,b illustrates the performance of the trained model on the full training set and the validation set, respectively, including all different types of samples. The model achieves an error of 0.69% on the validation data set. This demonstrates the potential of using deep learning techniques to predict moisture content based on material's electrochemical signals. In future studies, the inclusion of more data and further model adjustments will further enhance the reliability of the model. By integrating both the electrical and physical information in the model, the proposed approach significantly enhances the accuracy of moisture content prediction. The trained 1DCNN model can effectively analyze the complex relationship between the input signals and moisture content, enabling real-time and reliable monitoring without the need for further calibration.

Comparative Analysis of Model Performance. To better illustrate the advantages of our proposed model structure in moisture content sensing and to understand the role of each component, we conducted a comprehensive comparative analysis. Figure 6c succinctly illustrates the performance metrics of various predictive models applied to moisture content estimation in pharmaceutical samples. Linear regression, while foundational, exhibits limited efficacy, as indicated by its lower R^2 value and higher mean absolute error (MAE). This suggests that simplistic reliance on EIS indices and statistical measures is inadequate for complex moisture content dynamics. Subsequent implementations using impedance spectrum data to construct random forest regressors and neural networks showed some improvements. However, these models did not reach the high-performance threshold set by the 1DCNN architecture. The lackluster performance of these advanced models, compared to 1DCNN, accentuates the latter's sophisticated signal processing capabilities.

The training loss trends, as depicted in Figure S7 from the Supporting Information, provide insight into the learning dynamics of the neural network (NN) and the 1DCNN models. It is noteworthy that the NN model demonstrates a rapid decline in training loss, suggesting an initial quick adaptation to the patterns within the data set. This could be indicative of the model's simpler architecture, which may allow for faster convergence but potentially at the cost of overfitting or lack of generalizability. Conversely, the 1DCNN exhibits a more gradual reduction in loss over epochs. This slower convergence rate can be attributed to the model's more complex and nuanced structure, which is designed to capture spatial hierarchies in the spectroscopy data. The convolutional layers in the 1DCNN model process the data through multiple filters, which may initially slow down the learning process as the model begins to understand and learn the more intricate patterns in the frequency spectrum of the signals.

The pinnacle of accuracy is achieved with the introduction of the baseline mechanism within the 1DCNN structure, significantly enhancing the model's precision, as reflected by the highest R^2 (0.93) value and the lowest MAE (0.69%) in Figure 6c. This baseline channel, representing dry sample conditions, provides a reference point for the model, capturing intrinsic signal characteristics associated with different moisture levels. The incorporation of a baseline mechanism constitutes a paradigm shift, facilitating the 1DCNN's contextual processing of signals by differentiating between fluctuations attributable to moisture content and inherent baseline characteristics. Through extensive and methodical training, 1DCNN acquires the ability to discern and decode intricate patterns within the data, establishing direct associations with the precise moisture content values. The empirical data illustrated in the figure corroborate that this bifurcated channel strategy not only bolsters the efficiency of the learning process but also significantly enhances the predictive precision of the model.

Material-Specific Cross-Validation. In a departure from conventional random data splitting, our study implemented a methodical cross-validation technique predicated on the intentional separation of data based on material types. This method rigorously tests the model's ability to generalize and infer moisture content in new materials not included in the database. The performance metrics on the validation material data sets, as depicted in Figure 6d, are indicative of the model's generalization abilities. Remarkably, the results reveal that the inclusion of the baseline enhances the model's accuracy across different materials. The baseline provides the model with a reference to the initial, unaltered state of the materials, which is instrumental in distinguishing the precise moisture differentials. Consequently, this context-enriched analysis enables

https://doi.org/10.1021/acssensors.4c01180
ACS Sens. 2024, 9, 4186−4195

the model to make more informed decisions regarding moisture. This is a testament to the baseline's role in bolstering the model's interpretative framework, allowing it to effectively utilize the baseline characteristics as a comparative foundation for accurate moisture determination.

This approach to cross-validation not only underscores the robustness of the 1DCNN model but also confirms its potential for broader application in scenarios in which knowledge transfer to new material types is crucial. The success of this methodology paves the way for the adoption of calibration-free and efficient testing technologies within pharmaceutical production lines. It validates the model's proficiency in leveraging the inherent knowledge embedded within the EIS signals, marking a significant advancement in the domain of predictive moisture content analysis. Such calibration-free methods promise to streamline the analytical process, reduce downtime, and enhance the overall efficiency of pharmaceutical manufacturing, thereby ensuring consistent product quality and compliance with stringent regulatory standards.

CONCLUSIONS

In this study, we have demonstrated the potential of impedance spectroscopy as a reliable method for characterizing the moisture content in pharmaceutical materials. Through the utilization of impedance signals, we successfully investigated the correlation between electrical properties and varying moisture contents in pharmaceutical samples.

Through the utilization of equivalent circuit modeling, we successfully interpreted the mechanism underlying impedance spectroscopy's sensitivity to moisture content variations. The equivalent circuit analysis allowed us to identify key parameters that exhibited strong correlations with the actual moisture content of the samples. Leveraging AI techniques, we developed a 1DCNN model to process complex spectroscopy data effectively. By combining the frequency spectrum information, equivalent circuit indices, and material characteristics as inputs, our proposed model achieved remarkable results. The model's predictive capability produced a moisture content prediction model with an average error as low as 0.69%. This exceptional accuracy eliminates the need for calibration, providing a rapid and calibration-free solution for real-time moisture content monitoring in the pharmaceutical production process.

In summary, our study establishes impedance spectroscopy as a robust method for quantifying the moisture content in pharmaceutical materials. Furthermore, the methodologies and findings from this study have broader applications in other industries, such as food processing, agriculture, and electronics. Our study provides a pilot framework for exploring how deep learning can enhance sensor technologies through data-driven approaches, potentially extending its utility to diverse industries.

ASSOCIATED CONTENT

Data Availability Statement

Data will be made available upon reasonable request.

Supporting Information

The Supporting Information is available free of charge at https://pubs.acs.org/doi/10.1021/acssensors.4c01180.

Addition experimental details, including materials and deep learning model structure; method for model performance evaluation; representative sensing data; database development; and preanalysis (PDF)

AUTHOR INFORMATION

Corresponding Author

Yining Feng − *Lyles School of Civil and Construction Engineering, Sustainable Materials and Renewable Technology (SMART) Lab, Purdue University, West Lafayette, Indiana 47907-2051, United States; Center for Intelligent Infrastructures, Purdue University, West Lafayette, Indiana 47906, United States;* orcid.org/0000-0001-5683-0079; Email: feng109@purdue.edu

Authors

Guangshuai Han − *Lyles School of Civil and Construction Engineering, Sustainable Materials and Renewable Technology (SMART) Lab, Purdue University, West Lafayette, Indiana 47907-2051, United States;* orcid.org/0000-0001-9297-5072

Brent Maranzano − *Pfizer Worldwide Research &Development, Groton, Connecticut 06340, United States*

Christopher Welch − *Indiana Consortium for Analytical Science & Engineering, Indianapolis, Indiana 46202, United States;* orcid.org/0000-0002-8899-4470

Na Lu − *Lyles School of Civil and Construction Engineering, Sustainable Materials and Renewable Technology (SMART) Lab, Purdue University, West Lafayette, Indiana 47907-2051, United States; Center for Intelligent Infrastructures, Purdue University, West Lafayette, Indiana 47906, United States;* orcid.org/0000-0002-6367-1341

Complete contact information is available at: https://pubs.acs.org/10.1021/acssensors.4c01180

Author Contributions

G.H.: Writing, investigation, data curation, and data analysis. B.M.: Resources and methodology. C.W.: Project administration. N.L.: Methodology and review and editing. Y.F.: Supervision, funding acquisition, conceptualization, and review and editing.

Notes

The authors declare no competing financial interest.

ACKNOWLEDGMENTS

The authors acknowledge the funding support from NSF Center for Bioanalytical Metrology under Grant IIP-1916691.

REFERENCES

(1) Crouter, A.; Briens, L. The Effect of Moisture on the Flowability of Pharmaceutical Excipients. *AAPS PharmSciTech* **2014**, *15* (1), 65−74.

(2) Zhao, G.; Qian, F.; Li, X.; Tang, Y.; Sheng, Y.; Li, H.; Rao, J.; Singh, M. V.; Algadi, H.; Niu, M.; Zhang, W.; Guo, Z.; Peng, X.; Chen, T. Constructing a Continuous Reduced Graphene Oxide Network in Porous Plant Fiber Sponge for Highly Compressible and Sensitive Piezoresistive Sensors. *Adv. Compos Hybrid Mater.* **2023**, *6* (5), 1−12.

(3) Xu, Q.; Wu, Z.; Zhao, W.; He, M.; Guo, N.; Weng, L.; Lin, Z.; Taleb, M. F. A.; Ibrahim, M. M.; Singh, M. V.; Ren, J.; El-Bahy, Z. M. Strategies in the Preparation of Conductive Polyvinyl Alcohol Hydrogels for Applications in Flexible Strain Sensors, Flexible Supercapacitors, and Triboelectric Nanogenerator Sensors: An Overview. *Adv. Composites Hybrid Mater.* **2023**, *6*, 203.

(4) Huang, A.; Guo, Y.; Zhu, Y.; Chen, T.; Yang, Z.; Song, Y.; Wasnik, P.; Li, H.; Peng, S.; Guo, Z.; Peng, X. Durable Washable

Wearable Antibacterial Thermoplastic Polyurethane/Carbon Nanotube@silver Nanoparticles Electrospun Membrane Strain Sensors by Multi-Conductive Network. *Adv. Compos Hybrid Mater.* **2023**, *6* (3), 1−13.
(5) Zhu, L.; Wu, Q.; Mei, X.; Li, Y.; Yang, J. Paper-Based Microfluidic Sensor Array for Tetracycline Antibiotics Discrimination Using Lanthanide Metal−Carbon Quantum Dots Composite Ink. *Adv. Compos Hybrid Mater.* **2023**, *6* (6), 1−12.
(6) Gradinarsky, L.; Brage, H.; Lagerholm, B.; Björn, I. N.; Folestad, S. In Situ Monitoring and Control of Moisture Content in Pharmaceutical Powder Processes Using an Open-Ended Coaxial Probe. *Meas Sci. Technol.* **2006**, *17* (7), 1847−1853.
(7) Heng, P. W. S.; Loh, Z. H.; Liew, C. V.; Lee, C. C. Dielectric Properties of Pharmaceutical Materials Relevant to Microwave Processing: Effects of Field Frequency, Material Density, and Moisture Content. *J. Pharm. Sci.* **2010**, *99* (2), 941−957.
(8) Peters, J.; Bartscher, K.; Döscher, C.; Taute, W.; Höft, M.; Knöchel, R.; Breitkreutz, J. In-Line Moisture Monitoring in Fluidized Bed Granulation Using a Novel Multi-Resonance Microwave Sensor. *Talanta* **2017**, *170* (March), 369−376.
(9) Julrat, S.; Trabelsi, S. In-Line Microwave Reflection Measurement Technique for Determining Moisture Content of Biomass Material. *Biosyst. Eng.* **2019**, *188*, 24−30.
(10) Avila, C. R.; Ferré, J.; de Oliveira, R. R.; de Juan, A.; Sinclair, W. E.; Mahdi, F. M.; Hassanpour, A.; Hunter, T. N.; Bourne, R. A.; Muller, F. L. Process Monitoring of Moisture Content and Mass Transfer Rate in a Fluidised Bed with a Low Cost Inline MEMS NIR Sensor. *Pharm. Res.* **2020**, *37* (5), 84.
(11) He, R.; Lu, N. Luna. Unveiling the Dielectric Property Change of Concrete during Hardening Process by Ground Penetrating Radar with the Antenna Frequency of 1.6 and 2.6 GHz. *Cem. Concr. Compos.* **2023**, *144* (August), No. 105279.
(12) Dong, W.; Li, W.; Lu, N.; Qu, F.; Vessalas, K.; Sheng, D. Piezoresistive Behaviours of Cement-Based Sensor with Carbon Black Subjected to Various Temperature and Water Content. *Compos B Eng.* **2019**, *178* (June), 107488.
(13) He, R.; Nantung, T.; Olek, J.; Lu, N. Use of Dielectric Constant for Determination of Water-To-Cement Ratio (W/C) In Plastic Concrete: Part 2 Comparison Determined W/C Values by Ground Penetrating Radar (GPR) And Microwave Oven Drying Measurements. *ES Mater. Manufacturing* **2023**, *21*, No. 874.
(14) Sundaram, J.; Kandala, C. V.; Govindarajan, K. N.; Subbiah, J. Sensing of Moisture Content of In-Shell Peanuts by NIR Reflectance Spectroscopy. *J. Sens Technol.* **2012**, *02* (01), 1−7.
(15) Ji, W.; Viscarra Rossel, R. A.; Shi, Z. Accounting for the Effects of Water and the Environment on Proximally Sensed Vis-NIR Soil Spectra and Their Calibrations. *Eur. J. Soil Sci.* **2015**, *66* (3), 555−565.
(16) Sudduth, K. A.; Hummel, J. W. Soil Organic Matter, CEC, and Moisture Sensing with a Portable NIR Spectrophotometer. *Transactions of the ASAE* **1993**, *36* (6), 1571−1582.
(17) Eva Tavčar, E.; Turk, E.; Kreft, S. Simple Modification of Karl-Fischer Titration Method for Determination of Water Content in Colored Samples. *J. Anal. Methods Chem.* **2012**, *2012* (1), No. 379724.
(18) van de Voort, F. R.; Sedman, J.; Cocciardi, R.; Juneau, S. An Automated FTIR Method for the Routine Quantitative Determination of Moisture in Lubricants: An Alternative to Karl Fischer Titration. *Talanta* **2007**, *72* (1), 289−295.
(19) Gallina, A.; Stocco, N.; Mutinelli, F. Karl Fischer Titration to Determine Moisture in Honey: A New Simplified Approach. *Food Control* **2010**, *21* (6), 942−944.
(20) Li, X. B.*Impedance Spectroscopy for Manufacturing Control of Material Physical Properties* 2003, p 110.
(21) Nelson, S. O.; Guo, W. C.; Trabelsi, S.; Kays, S. J. Dielectric Spectroscopy of Watermelons for Quality Sensing. *Meas Sci. Technol.* **2007**, *18* (7), 1887−1892.
(22) Wang, J. R.; Choudhury, B. J. Remote Sensing of Soil Moisture Content over Bare Fields at 1.4 GHz Frequency. *J. Geophys. Res.: Oceans* **1980**, *86*, 5277−5282.
(23) Szypłowska, A.; Lewandowski, A.; Yagihara, S.; Saito, H.; Furuhata, K.; Szerement, J.; Kafarski, M.; Wilczek, A.; Majcher, J.; Woszczyk, A.; Skierucha, W. Dielectric Models for Moisture Determination of Soils with Variable Organic Matter Content. *Geoderma* **2021**, *401* (June), 115288.
(24) Szypłowska, A.; Lewandowski, A.; Jones, S. B.; Sabouroux, P.; Szerement, J.; Kafarski, M.; Wilczek, A.; Skierucha, W. Impact of Soil Salinity, Texture and Measurement Frequency on the Relations between Soil Moisture and 20 MHz−3 GHz Dielectric Permittivity Spectrum for Soils of Medium Texture. *J. Hydrol.* **2019**, *579* (September), No. 124155.
(25) Jose, M.; Oudebrouckx, G.; Bormans, S.; Veske, P.; Thoelen, R.; Deferme, W. Monitoring Body Fluids in Textiles: Combining Impedance and Thermal Principles in a Printed, Wearable, and Washable Sensor. *ACS Sens.* **2021**, *6* (3), 896−907.
(26) Islam, M.; Wahid, K. A.; Dinh, A. V.; Bhowmik, P. Model of Dehydration and Assessment of Moisture Content on Onion Using EIS. *J. Food Sci. Technol.* **2019**, *56* (6), 2814−2824.
(27) Ibba, P.; Falco, A.; Abera, B. D.; Cantarella, G.; Petti, L.; Lugli, P. Bio-Impedance and Circuit Parameters: An Analysis for Tracking Fruit Ripening. *Postharvest. Biol. Technol.* **2020**, *159* (August 2019), No. 110978.
(28) Ando, Y.; Mizutani, K.; Wakatsuki, N. Electrical Impedance Analysis of Potato Tissues during Drying. *J. Food Eng.* **2014**, *121* (1), 24−31.
(29) Grammatikos, S. A.; Ball, R. J.; Evernden, M.; Jones, R. G. Impedance Spectroscopy as a Tool for Moisture Uptake Monitoring in Construction Composites during Service. *Compos A Appl. Sci. Manuf.* **2018**, *105*, 108−117.
(30) Cheng, E. M.; Fareq, M.; Abdullah, F. S.; Wee, F. H.; Khor, S. F.; Lee, Y. S.; Afendi, M.; Shukry, M.; Shahriman, A. B.; Khairunizanm, W.; Liyana, Z. Y.Dielectric Spectroscopy of Pharmaceutical Drug (Paracetamol) Dosage in Water. In *RFM 2013 - 2013 IEEE International RF and Microwave Conference, Proceedings* 2013; pp 409−413.
(31) Dogan, H.; Basyigit, I. B.; Genc, A. Determination and Modelling of Dielectric Properties of the Cherry Leaves of Varying Moisture Content over 3.30−7.05 GHz Frequency Range. *J. Microwave Power Electromagnetic Energy* **2020**, *54* (3), 254−270.
(32) Kabir, H.; Khan, M. J.; Brodie, G.; Gupta, D.; Pang, A.; Jacob, M. V.; Antunes, E. Measurement and Modelling of Soil Dielectric Properties as a Function of Soil Class and Moisture Content. *J. Microwave Power Electromagnetic Energy* **2020**, *54* (1), 3−18.
(33) Wang, J.; Fan, L.; Zhou, Q.; Li, J.; Zhao, P.; Wang, Z.; Zhang, H.; Yan, S.; Huang, L. Rapid Determination of Meat Moisture Content Using Radio-Frequency Dielectric Measurement. *IEEE Access* **2018**, *6*, 51384−51391.
(34) Yebra, M.; Dennison, P. E.; Chuvieco, E.; Riaño, D.; Zylstra, P.; Hunt, E. R.; Danson, F. M.; Qi, Y.; Jurdao, S. A Global Review of Remote Sensing of Live Fuel Moisture Content for Fire Danger Assessment: Moving towards Operational Products. *Remote Sens. Environ.* **2013**, *136*, 455−468.
(35) Xia, D.; Zhang, X.; Oskay, C. Large-Deformation Reduced Order Homogenization of Polycrystalline Materials. *Comput. Methods Appl. Mech Eng.* **2021**, *387*, No. 114119.
(36) Xia, D.; Oskay, C. Reduced Order Mathematical Homogenization Method for Polycrystalline Microstructure with Microstructurally Small Cracks. *Int. J. Numer Methods Eng.* **2023**, *124* (14), 3166−3190.
(37) Feng, Y.; Yazawa, K.; Lu, N. High-Performance Conformal Thermoelectric Generator for Environmental Monitoring. *ACS Appl. Electron Mater.* **2022**, *4* (1), 197−205.
(38) Goodson, H. V.; Miller, R. A.; Lee, S.; Fridmanski, E. J.; Barron, E.; Pence, J.; Lieberman, M. Scentsor": A Whole-Cell Yeast Biosensor with an Olfactory Reporter for Low-Cost and Equipment-Free Detection of Pharmaceuticals. *ACS Sens* **2020**, *5* (10), 3025−3030.

https://doi.org/10.1021/acssensors.4c01180
ACS Sens. 2024, 9, 4186−4195

(39) Siuzdak, K.; Niedziałkowski, P.; Sobaszek, M.; Łęga, T.; Sawczak, M.; Czaczyk, E.; Dziąbowska, K.; Ossowski, T.; Nidzworski, D.; Bogdanowicz, R. Biomolecular Influenza Virus Detection Based on the Electrochemical Impedance Spectroscopy Using the Nanocrystalline Boron-Doped Diamond Electrodes with Covalently Bound Antibodies. *Sens Actuators B Chem.* **2019**, *280* (September 2018), 263−271.
(40) Delfino, J. R.; Pereira, T. C.; Costa Viegas, H. D.; Marques, E. P.; Pupim Ferreira, A. A.; Zhang, L.; Zhang, J.; Brandes Marques, A. L. A Simple and Fast Method to Determine Water Content in Biodiesel by Electrochemical Impedance Spectroscopy. *Talanta* **2018**, *179* (September 2017), 753−759.
(41) Li, L.; Chen, T.; Gao, X.; Peng, L. Unveiling the Impact of Carbonation Treatment on BOF Slag Hydration Activity: Formation and Development of the Barrier Layer. *Constr Build Mater.* **2024**, *436* (May), No. 136959.
(42) Qin, L.; Xie, Q.; Bao, J.; Sant, G.; Chen, T.; Zhang, P.; Niu, D.; Gao, X.; Bauchy, M. Investigation of Carbonation Kinetics in Carbonated Cementitious Materials by Reactive Molecular Dynamics Simulations. *ACS Sustainable Chem. Eng.* **2024**, *12*, 10075.
(43) Lu, S.; Yang, J.; Gu, Y.; He, D.; Wu, H.; Sun, W.; Xu, D.; Li, C.; Guo, C. Advances in Machine Learning Processing of Big Data from Disease Diagnosis Sensors. *ACS Sens* **2024**, *9* (3), 1134−1148.
(44) Wang, M.; Cetó, X.; Del Valle, M. A Sensor Array Based on Molecularly Imprinted Polymers and Machine Learning for the Analysis of Fluoroquinolone Antibiotics. *ACS Sens* **2022**, *7* (11), 3318−3325.
(45) Bhatt, A.; Ganatra, A. Explosive Weapons and ARms Detection with SIngular Classification (WARDIC) on Novel Weapon Dataset Using Deep Learning: Enhanced OODA (Observe, Orient, Decide, and Act) Loop. *Eng. Sci.* **2022**, *20*, 252−266.
(46) Sharma, D.; Kudva, V.; Patil, V.; Kudva, A.; Bhat, R. S. A Convolutional Neural Network Based Deep Learning Algorithm for Identification of Oral Precancerous and Cancerous Lesion and Differentiation from Normal Mucosa: A Retrospective Study. *Eng. Sci.* **2022**, *18*, 278−287.
(47) Pradeep, T.; Kumar, D. R.; Kumar, N.; Wipulanusat, W.; Keawsawasvong, S.; Sunkpho, J. Performance Evaluation and Triangle Diagram of Deep Learning Models for Embedment Depth Prediction in Cantilever Sheet Piles. *Eng. Sci.* **2024**, *28*, 1082.
(48) Luo, K.; Chen, X.; Zheng, H.; Shi, Z. A Review of Deep Learning Approach to Predicting the State of Health and State of Charge of Lithium-Ion Batteries. *J. Energy Chem.* **2022**, *74*, 159−173.
(49) Jenarthanan, M. P.; Harinesh, B.; Arunachalam, U. Modelling and Prediction of Machining Forces During End Milling of Glass Fibre Reinforced Polymer Composites Using Regression Analysis and Artificial Neural Networks (ANN). *Eng. Sci.* **2023**, *23*, 869.
(50) Paji, M. K.; Gordan, B.; Bedon, C.; Faridmehr, I.; Valerievich, K.; Hwang, H. J. Artificial Neural Network Levenberg-Marquardt Based Algorithm for Compressive Strength Estimation of Concrete Mixed with Magnetic Salty Water. *Eng. Sci.* **2023**, *23*, 1−11.
(51) Jawad, R. S.; Abid, H. Fault Detection and Classification for VSC-HVDC Systems by Using Different Swarm Optimization Algorithms-Based Neural Network. *Eng. Sci.* **2023**, *23*, 884.
(52) Bhat, P.; Shukla, T.; Naik, N.; Korir, D.; Randhawa, P.; Samrot, A. V.; Ramya, S.; Salmataj, S. A. Deep Neural Network as a Tool to Classify and Identify the 316L SS And AZ31BMg Metal Surface Morphology: An Empirical Study. *Eng. Sci.* **2023**, *26*, 1−14.
(53) Han, G.; Su, Y. F.; Nantung, T.; Lu, N. Mechanism for Using Piezoelectric Sensor to Monitor Strength Gain Process of Cementitious Materials with the Temperature Effect. *J. Intell Mater. Syst. Struct* **2021**, *32* (10), 1128−1139.
(54) Su, Y. F.; Han, G.; Nantung, T.; Lu, N. Novel Methodology on Direct Extraction of the Strength Information from Cementitious Materials Using Piezo-Sensor Based Electromechanical Impedance (EMI) Method. *Constr Build Mater.* **2020**, *259*, No. 119848.
(55) Liu, Y.; Xu, J.; Tao, Y.; Fang, T.; Du, W.; Ye, A. Rapid and Accurate Identification of Marine Microbes with Single-Cell Raman Spectroscopy. *Analyst* **2020**, *145* (9), 3297−3305.
(56) Akankasha Sinha, R. M. *Innovative Data Communication Technologies and Application*, 2019; Vol. *10*.
(57) Shao, Y.; Zhu, Y.; Zheng, R.; Wang, P.; Zhao, Z.; An, J. Highly Sensitive and Selective Surface Molecularly Imprinted Polymer Electrochemical Sensor Prepared by Au and MXene Modified Glassy Carbon Electrode for Efficient Detection of Tetrabromobisphenol A in Water. *Adv. Compos Hybrid Mater.* **2022**, *5* (4), 3104−3116.
(58) Vyas, S.; Shukla, A.; Shivhare, S.; Das, R.; Venkatesh, R. Core-Shell Structured Polyaniline (PANI) − Manganese Dioxide (MnO2) Nanocomposites as an Electrochemical Sensor for Detection of Emamectin Benzoate. *ES Mater. Manufact.* **2024**, *23*, 1−9.

https://doi.org/10.1021/acssensors.4c01180
ACS Sens. 2024, 9, 4186−4195